A Bolus Calculator Based on Continuous-Discrete Unscented Kalman Filtering for Type 1 Diabetics ⋆

Dimitri Boiroux [*,**] **Tinna Björk Aradóttir** [*]
Morten Hagdrup [*] **Niels Kjølstad Poulsen** [*] **Henrik Madsen** [*]
John Bagterp Jørgensen [*]

[*] *DTU Compute, Technical University of Denmark, Kgs. Lyngby, Denmark*
[**] *Danish Diabetes Academy, Odense, Denamrk*

Abstract: In patients with type 1 diabetes, the effects of meals intake on blood glucose level are usually mitigated by administering a large amount of insulin (bolus) at mealtime or even slightly before. This strategy assumes, among other things, a prior knowledge of the meal size and the postprandial glucose dynamics. On the other hand, administering the meal bolus during or after mealtime could benefit from the information provided by the postprandial meal dynamics at the expense of a delayed meal bolus. The present paper investigates different bolus administration strategies (at mealtime, 15 minutes after or 30 minutes after the beginning of the meal). We implement a continuous-discrete unscented Kalman filter to estimate the states and insulin sensitivity. These estimates are used in a bolus calculator. The numerical results demonstrate that administering the meal bolus 15 minutes after mealtime both reduces the risk of hypoglycemia in case of an overestimated meal and the time spent in hyperglycemia if the meal size is underestimated. Faster insulin and the use of glucagon will have the potential to encourage postprandial meal bolus administration and hence will not require to accurately estimate the meal size.

Keywords: Type 1 diabetes, Kalman filter, state estimation, parameter identification

1. INTRODUCTION

It is essential for patients with type 1 diabetes (T1D) to regulate their blood glucose tightly using frequent insulin injections, ideally in the range 4-8 mmol/L. Prolonged high blood glucose levels (hyperglycemia) may lead to long-term clinical complications, while low blood glucose levels have immediate effects.

An increasing number of patients use continuous glucose monitors (CGMs) and continuous subcutaneous infusion of insulin (CSII) pumps instead of multiple daily injections (MDI). This sensor- and pump- augmented therapy has proven to improve glycemic regulation compared to the conventional insulin therapy (Haidar et al. (2015)). Nevertheless, yet only a minority of patients using a CGM and CSII pump can manage to control their blood glucose level correctly according to the study by Nørgaard et al. (2013).

Automated or semi-automated control of blood glucose, also called the artificial pancreas (AP), has the potential to improve glycemic control and assist patients with T1D in their therapy. Current prototypes of the AP consist of a CGM, a control algorithm residing on a mobile platform (e.g. a smartphone) and a CSII pump. Fig. 1 illustrates
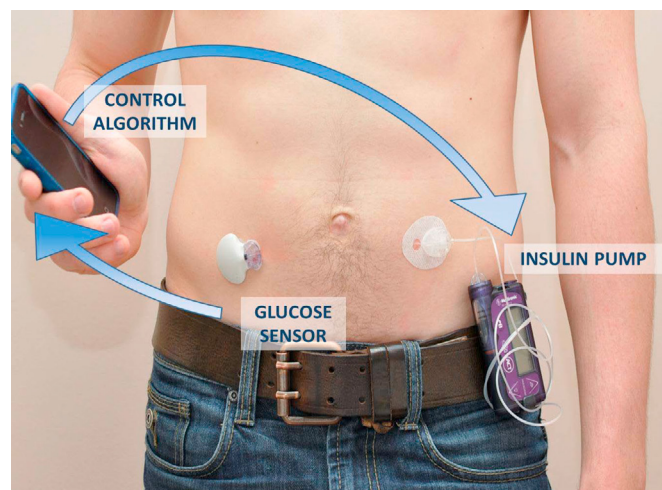

Fig. 1. The artificial pancreas.

the AP. Clinical studies demonstrated that the use of an AP during the night reduces the risk of nocturnal hypo- or hyperglycemia (Hovorka et al. (2010); Schmidt et al. (2013)). More recently, outpatient clinical studies were performed (Kovatchev et al. (2014)). However, tight glucose regulation during daytime is more difficult to achieve than during night time because of various disturbances that can affect the glucose level.

As a matter of fact, meals represent a major challenge both for the patient and the control algorithm due to the high nonlinearity of the insulin-glucose dynamics, the difficulty to accurately estimate the carbohydrates (CHO) content and the slower action of insulin compared to the meal intake. Brazeau et al. (2013) show the difficulty for patients with T1D to correctly estimate the CHO content of a given meal. An example illustrating the nonlinearity of glucose-insulin dynamics and the effects of the delayed insulin action on the postprandial glucose excursion can be found in Boiroux et al. (2010).

The current bolus calculators mainly rely on the patient ability to correctly estimate the meal size and the insulin-to-carbohydrates ratio. The computed bolus may then possibly be adjusted depending on the current glucose level and the estimated insulin on board

$$u_B = \frac{CHO}{ICR} + CF(G - \bar{G}) - IOB \qquad (1)$$

in which u_B [U] is the insulin bolus, CHO [g] is the estimated meal content, ICR [g/U] is the insulin-to-CHO ratio (the amount of CHO), CF [U/(mmol/L)] is the correction factor (the amount of insulin needed to decrease the blood glucose level by 1 mmol/L), G [mmol/L] is the current glucose level, $\bar{G}$ [mmol/L] is the target glucose level and IOB [U] is the estimated insulin on board (see e.g. Zisser et al. (2008) for a review of bolus calculators). In the case where the meal size and time are perfectly known, it is usually optimal to administer the meal bolus either at mealtime, or even before, excepted for meals with high-fat content (Srinivasan et al. (2014)). On the other hand, if the patient cannot estimate the meal size accurately, it may be preferable to estimate the bolus size based on the postprandial glucose dynamics.

In this paper, we want to investigate whether it is preferable to administer the meal bolus at mealtime and rely solely on the meal announcement provided by the patient, or to use the information provided by the postprandial dynamics - here, we consider waiting for 15 or 30 minutes. Waiting will provide a more accurate information about the CHO contents of the meals at the expense of a delayed bolus administration.

This paper proposes an approach based on a continuous-discrete unscented Kalman filter (CDUKF) to estimate the current states and parameters of the system. This estimate is used to compute the optimal prandial bolus in patient with T1D. The CDUKF has already been tested on the Bergman minimal model (Eberle and Ament (2012)) and on the Hovorka model (Szalay et al. (2014)). It is structured as following. Section 2 presents the physiological model of the patient used for simulation. Section 3 describes the continuous-discrete filter algorithm and its implementation. Section 4 introduces the bolus calculator. Section 5 discusses the simulation results for a population of 10 patients with T1D. Finally, section 6 summarizes the main findings of this paper.

2. PHYSIOLOGICAL MODEL

Several models describing the insulin-glucose dynamics and the CHO absorption have been developed, see e.g. Hovorka et al. (2004) or Cobelli et al. (2009). More recent models also include a description of the glucagon-glucose

dynamics, see Herrero et al. (2013) or Dalla Man et al. (2014). In this paper, we use the Medtronic Virtual Patient (MVP) model presented in Kanderian et al. (2009). This model has the main advantage to be easier to identify compared to the others, and therefore more suitable for the design of state and parameter estimators. It has been identified for 10 patients. The parameters for these 10 patients are used for the numerical simulations.

2.1 Insulin absorption subsystem

The insulin absorption subsystem is given by the following two-compartment model

$$\frac{dI_{SC}}{dt}(t) = \frac{u(t)}{C_I \tau_1} - \frac{I_{SC}(t)}{\tau_1} \qquad (2a)$$

$$\frac{dI_P}{dt}(t) = \frac{I_{SC}(t) - I_P(t)}{\tau_2} \qquad (2b)$$

where $I_{SC}(t)$ [mU/L/min] is the subcutaneous insulin concentration, and $I_P(t)$ [mU/L] is the plasma insulin concentration. $u(t)$ [mU/min] in the insulin infusion rate, C_I [L/min] is the clearance rate. τ_1 and τ_2 [min] are the insulin absorption time constants. It must be pointed out that these time constants are interchangeable.

2.2 Insulin-glucose dynamics

In the MVP model, the effect of insulin on blood glucose is described by the following ODEs

$$\frac{dI_{EFF}}{dt}(t) = -p_2 I_{EFF}(t) + p_2 S_I I_P(t) \qquad (3a)$$

$$\frac{dG}{dt}(t) = -(I_{EFF} + GEZI)G(t) + EGP + R_A(t) \qquad (3b)$$

$I_{EFF}(t)$ [min^{-1}] is the effect of insulin. p_2 [min^{-1}] is a parameter and S_I [mL/mU] reflects the insulin sensitivity. The glucose concentration $G(t)$ [mg/dL] is also affected by the glucose elimination at zero insulin rate ($GEZI$) [min^{-1}], the endogenous glucose production (EGP) [mg/dL/min] and the glucose rate of appearance $R_A(t)$ [mg/dL/min].

The insulin effect and the glucose dynamics (3) are similar to the one developed by Bergman et al. (1981). This formulation allows for an easier parameter identification compared to other physiological models.

2.3 Meal absorption subsystem

We consider here the two-compartment model used in Hovorka et al. (2004) to describe the CHO absorption and conversion to glucose. The model describes the effect of orally ingested carbohydrates on the rate of appearance of glucose $R_A(t)$ [mg/dL/min] in the blood stream. The model is

$$\frac{dD_1}{dt}(t) = d(t) - \frac{D_1(t)}{\tau_G} \qquad (4a)$$

$$\frac{dD_2}{dt}(t) = \frac{D_1(t) - D_2(t)}{\tau_G} \qquad (4b)$$

$$R_A(t) = \frac{D_2(t)}{\tau_G V_G} \qquad (4c)$$

$d(t)$ [mg/min] is the meal intake. τ_G [min] is the meal absorption time constant and V_G [dL^{-1}] is the glucose distribution volume.

2.4 Sensor model

In this paper, we use the model developed by Facchinetti et al. (2014) for a DEXCOM Seven Plus sensor. This model represents the glucose transport from plasma to interstitial tissues and the sensor noise. The glucose transport is modeled as

$$\frac{dG_{SC}}{dt}(t) = \frac{1}{\tau_{G,SC}}\left(G(t) - G_{SC}(t)\right) \tag{5}$$

where the time constant $tau_{G,SC}$ is 6.7 min.

Then, the noise is represented by the sum of the two following autoregressive processes

$$cc(t) = 1.23cc(t-1) - 0.3995cc(t-2) + w_{cc}(t) \tag{6a}$$
$$\hat{v}(t) = 1.013\hat{v}(t-1) - 0.2135\hat{v}(t-2) + w(t) \tag{6b}$$

in which $cc(t)$ is the noise from the common component, $\hat{v}(t)$ is the measurement noise, $w_{cc}(t) \sim N(0,11.3$ mg^2/dL^2) and $w(t) \sim N(0,14.45$ mg^2/dL^2).

3. THE CONTINUOUS-DISCRETE UNSCENTED KALMAN FILTER (CDUKF)

The unscented Kalman filter (UKF) has been developed by Julier et al. (2000). In many applications, this filter shows better performance than the extended Kalman filter (EKF) without increasing the computational time order. The UKF propagates the state and covariance estimates for a set of wisely chosen points (also called sigma points) such that the nonlinearities are more accurately propagated than for the EKF. The UKF has been applied to plasma insulin estimation based on glucose measurements, see Eberle and Ament (2011).

However, this filter was initially designed for discrete-time systems. Sarkka (2007) presents a continuous-time and continuous-discrete unscented Kalman filter (CDUKF). This section recalls the principle and the implementation of the CDUKF and describes its application for state and parameter estimation.

The CDUKF estimates the states of the system given a stochastic continuous-time model and measurements at discrete times, i.e.

$$dx(t) = f(t, x(t), u(t), \theta)dt + \sigma d\omega(t) \tag{7a}$$
$$y_k = h(t_k, x(t_k)) + v_k \tag{7b}$$

in which $x(t)$ is the state vector. $u(t)$ is the input vector. Here, we assume a zero-order hold parametrization, i.e. $u(t) = u_k$ for $t_k \leq t < t_{k+1}$. θ represents the model parameters. $\{\omega(t),\ t \geq 0\}$ is a standard Wiener process with covariance Idt. We assume that the matrix σ is time-invariant. The measurement noise v_k is normally distributed, $v_k \sim N_{iid}(0, R_k)$.

We assume that the initial state x_0 is normally distributed with a known mean and covariance, $x_0 \sim N(\hat{x}_{0|-1}, P_{0|-1})$.

3.1 Prediction step

For any integer $k \geq 1$, we consider the following sigma points

$$\mathcal{X}_{k-1} = \left[\hat{x}_{k-1}\ \hat{x}_{k-1} \pm \gamma\sqrt{P_{k-1}}\right] \tag{8}$$

where $\gamma = \sqrt{L + \lambda}$. The parameter $\lambda = \alpha^2(L + \kappa) - L$ is a scaling parameter. The tuning parameter $0 \leq \alpha < 1$ has an influence on the spread of the sigma points around the mean value and is usually set to a small value. Here, we choose $\alpha = 10^{-4}$. A square root of P_{k-1} (which is in the general case not unique) can for example be computed by using the Cholesky factorization.

The weights $W_i^{m,c}$ are defined as

$$W_0^m = \frac{\lambda}{L + \lambda} \tag{9a}$$

$$W_0^c = \frac{\lambda}{L + \lambda} + 1 - \alpha^2 + \beta \tag{9b}$$

$$W_i^m = W_i^c = \frac{1}{2(L + \lambda)}, \quad i = 1, 2, ..., 2L \tag{9c}$$

Here, we set $\beta = 2$ since we assume that the process and output noises follow a Gaussian distribution. Furthermore, we define

$$w_m = [W_0^m\ W_1^m\ \cdots\ W_{2L}^m]' \tag{10a}$$
$$W = (I - [w_m\ \cdots\ w_m])\,\mathrm{diag}\left(W_0^c \cdots W_{2L}^c\right)$$
$$(I - [w_m\ \cdots\ w_m])' \tag{10b}$$

The one-step ahead prediction of the mean-covariance is determined by solving the following system of differential equations for $t_{k-1} \leq t \leq t_k$

$$\frac{d\hat{x}}{dt}(t) = f(\mathcal{X}(t), u(t), \theta)w_m \tag{11a}$$
$$\frac{dP(t)}{dt} = \mathcal{X}(t)Wf(\mathcal{X}(t), u(t), \theta)' +$$
$$f(\mathcal{X}(t), u(t), \theta)W\mathcal{X}(t)' + \sigma\sigma' \tag{11b}$$

with the initial conditions $\hat{x}(t_{k-1}) = \hat{x}_{k-1}$ and $P(t_{k-1}) = P_{k-1}$. The one-step ahead prediction of the output is

$$\hat{y}_k^- = h(t_k, \mathcal{X}_k^-)w_m \tag{12}$$

3.2 Filtering step

Since we have discrete outputs, the filtering step is similar to the discrete UKF. The mean variance and covariance of the process and output noise are

$$P_{x_k y_k} = \mathcal{X}_k^- W h(t_k, \mathcal{X}_k^-)' \tag{13a}$$
$$P_{\tilde{y}_k \tilde{y}_k} = h(t_k, \mathcal{X}_k^-)W h(t_k, \mathcal{X}_k^-)' \tag{13b}$$

Similarly to the extended Kalman filter, the Kalman gain is

$$K_k = P_{x_k y_k} P_{\tilde{y}_k \tilde{y}_k}^{-1} \tag{14}$$

and the filtered mean and process covariance are

$$\hat{x}_k = \hat{x}_{k-1} + K_k\left(y_k - \hat{y}_k^-\right) \tag{15a}$$

Further explanations about the CDUKF can be found in Sarkka (2007).

3.3 Parameter estimation

We perform online parameter estimation by augmenting the states with the set of parameters we want to estimate. The continuous-time SDE system becomes

$$\begin{bmatrix} dx(t) \\ d\theta(t) \end{bmatrix} = \begin{bmatrix} f(t, x(t), u(t)) \\ 0 \end{bmatrix} dt + \bar{\sigma}d\omega(t) \tag{16}$$

where $\theta(t)$ is the set of parameters we want to estimate and $\bar{\sigma}d\omega(t)$ represents the augmented Wiener process. The filtering and one-step ahead prediction steps presented

previously are then modified accordingly. In our case, we want to estimate the insulin sensitivity $S_I(t)$ and the meal compartment $D_1(t)$.

Nevertheless, these two states cannot be estimated simultaneously. For instance, if a sudden increase in blood glucose level occurs, it can be either attributed to a change in patient's physiology (e.g. an increased resistance to insulin) or to a meal intake. We use the following switching strategy to estimate these two states:

- If no meal has been ingested within the three previous hours, the filter will only estimate the insulin sensitivity $S_I(t)$.
- If a meal has been ingested within the three previous hours, the filter will only estimate the meal compartment $D_1(t)$.

4. BASAL AND BOLUS CALCULATION

Meals are the major disturbance for blood glucose in patients with T1D. Therefore, a possible approach is to handle them in a different way. For instance feedforward-feedback control assumes that the estimated meal size is announced to the controller (Abu-Rmileh and Garcia-Gabin (2010); Boiroux et al. (2011)). In this approach, the insulin administration can be separated between basal insulin and insulin boluses. Basal insulin must compensate for endogenous glucose production. It is determined by determining the steady state of the model, and must be adjusted to reflect the intra-patient variability. Insulin boluses are used to mitigate the postprandial glucose excursion. The bolus size is determined by the state estimate and the meal size announced by the patient.

At each time sample, the basal insulin infusion rate $u_{ss,k}$ is determined by solving the nonlinear system of equations

$$f(x(t), u_{ss,k}, 0) = 0 \tag{17}$$

for the glucose level $G_0 = 6\text{mmol/L}$.

When a meal is announced to the controller (or 15 or 30 minutes after the meal is announced) at a given time t_k, the optimal bolus and the optimal postprandial blood glucose trajectory are computed by solving the univariate constrained optimization problem

$$\min_{u^{bolus}} \psi = \frac{1}{2} \sum_{j=0}^{N-1} \| \max(\hat{y}_{j+k+1} - \bar{G}, 0)\|_2^2 +$$
$$\kappa \| \max(\bar{G} - \hat{y}_{j+k+1}, 0)\|_2^2 \tag{18a}$$

$$s.t. \quad \dot{x}(t) = f(x(t), u_{j+k}, d_{j+k}) \quad t \in [t_{j+k}, t_{j+k+1}[\tag{18b}$$

$$x_0 = \hat{x}_k \tag{18c}$$

$$u_0 = u_{ss,k} + u^{bolus} \tag{18d}$$

$$u_{j+k} = u_{ss,k}, \quad j = 0, 1, \ldots, N-1 \tag{18e}$$

$$y_{j+k} = Cx_{j+k} \tag{18f}$$

The parameter $\kappa = 10^4$ heavily penalizes glucose levels below $\bar{G} = 4.5$ mmol/L. In other words, we want to find the optimal bolus such that the reference signal is close to the desired glucose target $\bar{G}$ for all times. In this case, the predictions on the future states of the system are made using the continuous-time nonlinear model.

5. NUMERICAL RESULTS AND DISCUSSION

5.1 Scenario Description

We compare different bolus administration strategies for the 10 patients identified in Kanderian et al. (2009) for three-day simulations. Each day comprises 3 meals (70g CHO at 6AM, 75g CHO at noon, 75g CHO at 6PM). We consider the three following strategies for bolus administration (for the simulations, we assume that the meal is instantly consumed)

- The bolus is administered at mealtime (T+0 min)
- The bolus is administered 15 minutes after mealtime (T+15 min)
- The bolus is administered 30 minutes after mealtime (T+30 min)

and for each strategy, we consider the cases where the mealsize is underestimated by 50%, correctly estimated or overestimated by 50%. We also double the insulin sensitivity parameter S_I in (3a) to challenge the parameter estimation of the CDUKF.

We use the 10 patients identified in Kanderian et al. (2009) and the CGM model described in section 2.4 to generate a population of patients with type 1 diabetes. We use the same CGM noise for all patients and all simulations for comparison purposes.

5.2 Numerical Results

Table 1 illustrates the median time spent in hyperglycemia, within target or in hypoglycemia for each case. In the case where patients underestimate the meal, late administration of insulin increases the time in target. Looking at individual statistics shows that 5 patients out of 10 reduce their time spent in hyperglycemia if they administer their meal bolus after 15 minutes instead of administering it at mealtime, and 3 out of 10 reduce the time spent in hyperglycemia if they administer their meal bolus after 30 minutes (data not shown). No hypoglycemic event (i.e. glucose levels below 3.9 mmol/L) were observed.

In the case where the exact meal size is known, the insulin administration at mealtime is optimal. Later administration of insulin increases the time spent in hyperglycemia. Again, no hypoglycemic event were observed. This result is in line with previous studies establishing that administering the bolus at mealtime is optimal in the case where the meal size is known.

Finally, in the case where the meal size is overestimated by 50%, waiting before administering the bolus helps to reduce the time spent in hypoglycemia. In our simulations, even a large overestimation of the meal size does not induce severe hypoglycemia (i.e. glucose levels below 3.5 mmol/L).

Glucagon can also be used as a safety hormone in case of overbolused meal. Recent studies on virtual patients and *in vivo* established that this hormone can reduce the severity of hypoglycemic events and the time spent in hypoglycemia (El-Khatib et al. (2010); Bátora et al. (2014)). Due to the nature of the insulin profiles, it may be expected that an insulin administration strategy

Table 1. Summary of the results for all the 10 patients - median (interquartile range).

		T+0 min	T+15 min	T+30 min
Underestimated meal size by 50%	$G > 10$ mmol/L (%)	18.1 (4.9-32.1)	19.2 (8.9-31.1)	20.7 (10.5-31.6)
	$8 \leq G \leq 10$ mmol/L (%)	14.1 (10.8-21.4)	13.1 (8.5-19.9)	11.6 (8.5-18.7)
	$3.9 \leq G \leq 8$ mmol/L (%)	63.1 (44.4-73.7)	63.8 (49.3-72.5)	63.5 (51.9-72.7)
	$G < 3.9$ mmol/L (%)	0 (0-0)	0 (0-0)	0 (0-0)
	Daily insulin administered (U)	40.8 (27.6-51.6)	41.1 (28.0-51.6)	41.3 (29.2-53.5)
Correct meal size	$G > 10$ mmol/L (%)	14.7 (0-28.6)	17.0 (0-29.4)	19.7 (11.9-32.1)
	$8 \leq G \leq 10$ mmol/L (%)	11.8 (8.5-14.1)	11.8 (8.1-18.0)	12.1 (8.6-18.8)
	$3.9 \leq G \leq 8$ mmol/L (%)	66.6 (55.6-87.7)	65.9 (54.8-80.2)	62.9 (50.9-72.4)
	$G < 3.9$ mmol/L (%)	0 (0-0)	0 (0-0)	0 (0-0)
	Daily insulin administered (U)	42.4 (30.8-58.7)	42.0 (29.9-56.3)	41.0 (29.0-52.6)
Overestimated meal size by 50%	$G > 10$ mmol/L (%)	11.4 (0-25.7)	15.4 (0-28.5)	18.4 (1.5-31.3)
	$8 \leq G \leq 10$ mmol/L (%)	9.3 (6.0-13.6)	11.2 (7.9-13.6)	10.4 (7.4-14.5)
	$3.9 \leq G \leq 8$ mmol/L (%)	71.3 (65.2-88.8)	72.1 (62.9)	69.4 (60.0-84.1)
	$G < 3.9$ mmol/L (%)	0 (0-0.4)	0 (0-0)	0 (0-0)
	Daily insulin administered (U)	44.5 (32.6-66.5)	42.7 (31.1)-62.1	41.5 (29.2-55.8)

using frequent CGM measurements and a smart pen could perform as well as the one using a CGM and a CSII pump. Even in this case, a bolus administration of glucagon could be envisaged, if needed.

Fig. 2 shows the glucose and insulin traces for one patient in the case where the meal size is underestimated by 50% (Fig. 2(a)), correctly estimated (Fig. 2(b)) and overestimated by 50% (Fig. 2(c)). These figures show that the bolus size computed by the UKF is not proportional to the meal size due to the nonlinearity in glucose-insulin dynamics, even in the case where the bolus is administered at mealtime. This shows that the bolus calculator based on UKF will be less sensitive to mismatch in meal announcement compared to the conventional bolus calculator (1).

6. CONCLUSION

The method presented in this paper suggests that waiting before administering the meal bolus can reduce the time spent outside the target in the case where the meal size cannot be accurately estimated, or can efficiently reduce the effects of a missed bolus. Also, a sensor-augmented therapy combined with a smart pen could perform similarly as a sensor- and pump-augmented insulin therapy, but would be less flexible. Novel technologies, such as glucagon analogues stable in liquid solution, as well as faster insulin analogues, more accurate CGMs and better filtering algorithms will make late bolus insulin administration more beneficial in the future.

REFERENCES

Abu-Rmileh, A. and Garcia-Gabin, W. (2010). Feedforward-feedback multiple predictive controllers for glucose regulation in type 1 diabetes. *Computer Methods and Programs in Biomedicine*, 99, 113–123.

Bátora, V., Tárnik, M., Murgaš, J., Schmidt, S., Nørgaard, K., Poulsen, N.K., Madsen, H., and Jørgensen, J.B. (2014). Bihormonal model predictive control of blood glucose in people with type 1 diabetes. In *2014 IEEE Multi-Conference on Systems and Control (MSC)*.

Bergman, R.N., Phillips, L.S., and Cobelli, C. (1981). Physiologic evaluation of factors controlling glucose tolerance in man: measurement of insulin sensitivity and beta-cell glucose sensitivity from the response to intravenous glucose. *Journal of Clinical Investigation*, 68(6), 1456 – 1467.

Boiroux, D., Finan, D.A., Jørgensen, J.B., Poulsen, N.K., and Madsen, H. (2011). Strategies for glucose control in people with type 1 diabetes. In *Proceedings of the 18th World Congress, The International Federation of Automatic Control*, 3765–3770.

Boiroux, D., Finan, D.A., Poulsen, N.K., Madsen, H., and Jørgensen, J.B. (2010). Optimal insulin administration for people with type 1 diabetes. In *Proceedings of the 9th International Symposium on Dynamics and Control of Process Systems (DYCOPS 2010)*, 234 – 239.

Brazeau, A., Mircescu, H., Desjardins, K., Leroux, C., Strychar, I., Ekoé, J., and Rabasa-Lhoret, R. (2013). Carbohydrate counting accuracy and blood glucose variability in adults with type 1 diabetes. *Diabetes research and clinical practice*, 99(1), 19–23.

Cobelli, C., Dalla Man, C., Sparacino, G., Magni, L., De Nicolao, G., and Kovatchev, B.P. (2009). Diabetes: Models, signals, and control. *IEEE Reviews in Biomedical Engineering*, 2, 54–96.

Dalla Man, C., Micheletto, F., Lv, D., Breton, M., Kovatchev, B., and Cobelli, C. (2014). The UVA/PADOVA type 1 diabetes simulator new features. *Journal of diabetes science and technology*, 8(1), 26–34.

Eberle, C. and Ament, C. (2011). The unscented Kalman filter estimates the plasma insulin from glucose measurement. *Biosystems*, 103(1), 67–72.

Eberle, C. and Ament, C. (2012). Real-time state estimation and long-term model adaptation: a two-sided approach toward personalized diagnosis of glucose and insulin levels. *Journal of diabetes science and technology*, 6(5), 1148–1158.

El-Khatib, F., Russell, S., Nathan, D., Sutherlin, R., and Damiano, E. (2010). A bihormonal closed-loop artificial pancreas for type 1 diabetes. *Science Translational Medicine*, 2(27), 27ra27.

Facchinetti, A., Del Favero, S., Sparacino, G., Castle, J.R., Ward, W.K., and Cobelli, C. (2014). Modeling the glucose sensor error. *IEEE Transactions on Biomedical Engineering*, 61(3), 620 – 629.

Haidar, A., Legault, L., Messier, V., Mitre, T.M., Leroux, C., and Rabasa-Lhoret, R. (2015). Comparison of dual-hormone artificial pancreas, single-hormone artificial pancreas, and conventional insulin pump therapy for glycaemic control in patients with type 1 diabetes: an open-label randomised controlled crossover trial. *The Lancet Diabetes & Endocrinology*, 3(1), 17–26.
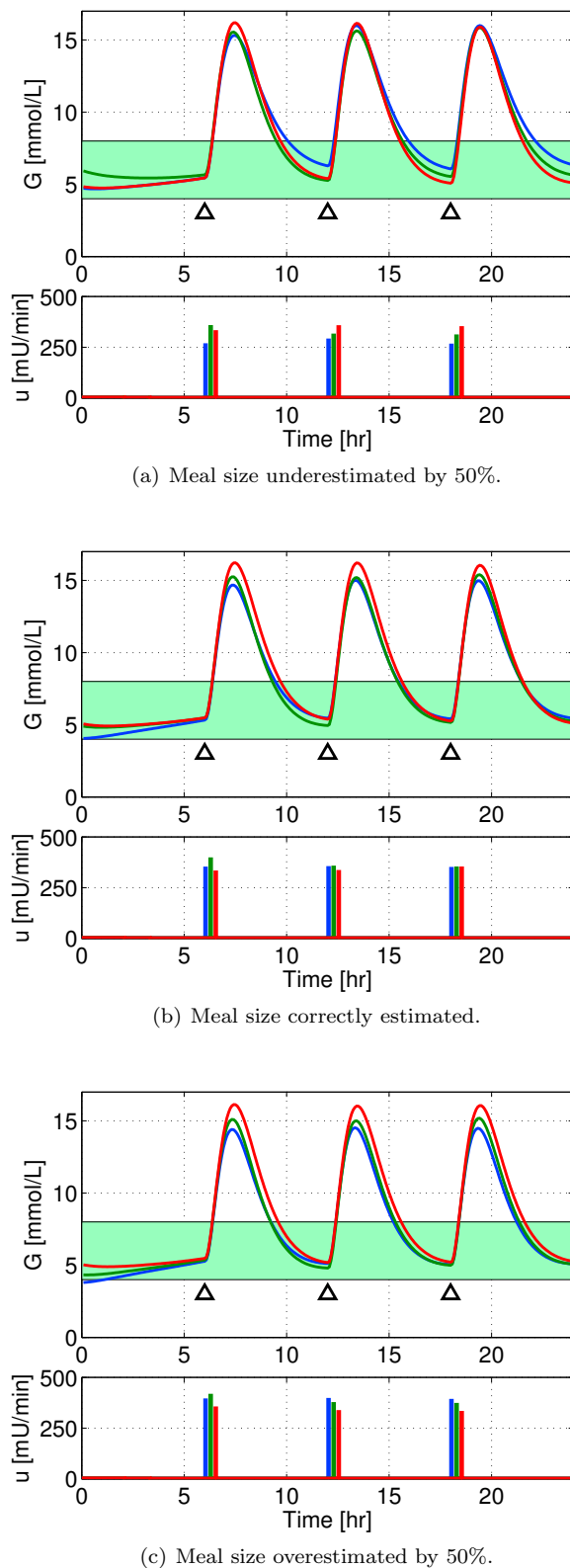
(a) Meal size underestimated by 50%.

(b) Meal size correctly estimated.

(c) Meal size overestimated by 50%.

Fig. 2. Glucose and insulin traces for a specific patient. The sampling time is 5 minutes. The insulin sensitivity S_I is twice its nominal value. Green-shaded area: Euglycemic range. Blue curve: T+0 min. Green curve: T+15 min. Red curve: T+30 min. Black triangles: Meals.

Herrero, P., Georgiou, P., Oliver, N., Reddy, M., Johnston, D., and Toumazou, C. (2013). A Composite Model of Glucagon-Glucose Dynamics for In Silico Testing of Bihormonal Glucose Controllers. *Journal of Diabetes Science and Technology*, 7(4), 941–951.

Hovorka, R., Allen, J.M., Elleri, D., Chassin, L.J., Harris, J., Xing, D., Kollman, C., Hovorka, T., Larsen, A.M.F., Nodale, M., De Palma, A., Wilinska, M.E., Acerini, C.L., and Dunger, D.B. (2010). Manual closed-loop insulin delivery in children and adolescents with type 1 diabetes: a phase 2 randomised crossover trial. *Lancet*, 375, 743 – 751.

Hovorka, R., Canonico, V., Chassin, L.J., Haueter, U., Massi-Benedetti, M., Federici, M.O., Pieber, T.R., Schaller, H.C., Schaupp, L., Vering, T., and Wilinska, M.E. (2004). Nonlinear model predictive control of glucose concentration in subjects with type 1 diabetes. *Physiological Measurement*, 25, 905–920.

Julier, S.J., Uhlmann, J.K., and Durrant-Whyte, H.F. (2000). A new method for the nonlinear transformation of means and covariances in filters and estimators. *IEEE Transactions on Automatic Control*, 45(3), 477–482.

Kanderian, S.S., Weinzimer, S., Voskanyan, G., and Steil, G.M. (2009). Identification of intraday metabolic profiles during closed-loop glucose control in individuals with type 1 diabetes. *Journal of Diabetes Science and Technology*, 3(5), 1047 – 1057.

Kovatchev, B.P., Renard, E., Cobelli, C., Zisser, H.C., Keith-Hynes, P., Anderson, S.M., Brown, S.A., Chernavvsky, D.R., Breton, M.D., Mize, L.B., et al. (2014). Safety of outpatient closed-loop control: first randomized crossover trials of a wearable artificial pancreas. *Diabetes care*, 37(7), 1789–1796.

Nørgaard, K., Scaramuzza, A., Bratina, N., Lalić, N.M., Jarosz-Chobot, P., Kocsis, G., Jasinskiene, E., Block, C.D., Carrette, O., Castañeda, J., et al. (2013). Routine sensor-augmented pump therapy in type 1 diabetes: the INTERPRET study. *Diabetes technology & therapeutics*, 15(4), 273–280.

Sarkka, S. (2007). On unscented kalman filtering for state estimation of continuous-time nonlinear systems. *IEEE Transactions on Automatic Control*, 52(9), 1631–1641.

Schmidt, S., Boiroux, D., Duun-Henriksen, A.K., Frøssing, L., Skyggebjerg, O., Jørgensen, J.B., Poulsen, N.K., Madsen, H., Madsbad, S., and Nørgaard, K. (2013). Model-based closed-loop glucose control in type 1 diabetes: The DiaCon experience. *Journal of Diabetes Science and Technology*, 7(5), 1255–1264.

Srinivasan, A., Lee, J.B., Dassau, E., and Doyle, F.J. (2014). Novel insulin delivery profiles for mixed meals for sensor-augmented pump and closed-loop artificial pancreas therapy for type 1 diabetes mellitus. *Journal of diabetes science and technology*, 8(5), 957 – 968.

Szalay, P., Molnar, A., Muller, M., Eigner, G., Rudas, I., Benyo, Z., and Kovacs, L. (2014). Comparison of sigma-point filters for state estimation of diabetes models. In *2014 IEEE International Conference on Systems, Man and Cybernetics (SMC)*, 2476–2481.

Zisser, H., Robinson, L., Bevier, W., Dassau, E., Ellingsen, C., Doyle III, F.J., and Jovanovic, L. (2008). Bolus calculator: a review of four smart insulin pumps. *Diabetes technology & therapeutics*, 10(6), 441–444.